

Photon energy lifter

Zeno Gaburro, Mher Ghulinyan, Francesco Riboli and Lorenzo Pavesi

Department of Physics, University of Trento and CNR-INFM, Povo, I-38050 Trento, Italy

Alessio Recati^a and Iacopo Carusotto

CRS BEC-INFM, Povo, I-38050 Trento, Italy

^a also at ECT*, Villazzano, Trento, Italy

gaburro@science.unitn.it

Abstract: We propose a time-dependent, spatially periodic photonic structure which is able to shift the carrier frequency of an optical pulse which propagates through it. Taking advantage of the slow group velocity of light in periodic photonic structures, the wavelength conversion process can be performed with an efficiency close to 1 and without affecting the shape and the coherence of the pulse. Quantitative Finite Difference Time Domain simulations are performed for realistic systems with optical parameters of conventional silicon technology.

© 2006 Optical Society of America

OCIS codes: (190.2620) Frequency conversion, (230.7370) Waveguides, (320.7080) Ultrafast devices, (230.7020) Traveling-wave devices

References and links

1. S. J. B. Yoo, "Wavelength Conversion Technologies for WDM Network Applications," *J. Lightwave Technol.* **14**, 955 (1996).
2. C. Q. Xu, H. Okayama, and M. Kawahara, "1.5 μm band efficient broadband wavelength conversion by difference frequency generation in a periodically domain-inverted LiNbO_3 channel waveguide," *Appl. Phys. Lett.* **63**, 3559 (1993).
3. T. Durhuus, B. Mikkelsen, C. Joergensen, S. L. Danielsen, and K. E. Stubkjaer, "All-Optical Wavelength Conversion by Semiconductor Optical Amplifiers," *J. Lightwave Technol.* **14**, 942 (1996).
4. M.F. Yanik, S. Fan, "Dynamic Photonic Structures: Stopping, Storage and Time Reversal of Light," *Studies in Applied Mathematics* **115**, 233–253 (2005).
5. M.F. Yanik, W. Suh, Z. Wang, and S. Fan, "Stopping Light in a Waveguide with an All-Optical Analog of Electromagnetically Induced Transparency," *Phys. Rev. Lett.* **93**, 233903 (2004)
6. M.F. Yanik and S. Fan, "Stopping and storing light coherently," *Phys. Rev. A* **71**, 013803 (2005)
7. M. L. Povinelli, S. G. Johnson, J. D. Joannopoulos, "Slow-light, band-edge waveguides for tunable time delays," *Opt. Express* **13**, 7145-7159 (2005).
8. C. Klingshirn, *Semiconductor Optics* (Springer-Verlag, Heidelberg, 1997)
9. K.J. Vahala, "Optical microcavities," *Nature* **424**, 839 (2003)
10. B.S. Song, S. Noda, T. Asano and Y. Akahane, "Ultra-high-Q photonic double-heterostructure nanocavity," *Nature Materials* **4**, 207 (2005).
11. M. Notomi and S. Mitsugi, "Wavelength conversion via dynamic refractive index tuning of a cavity," *Phys. Rev. A* **73**, 051803 (2006)
12. H. Gersen *et al.*, "Real-Space Observation of Ultraslow Light in Photonic Crystal Waveguides," *Phys. Rev. Lett.* **94**, 073903 (2005).
13. see, e.g., A. Melloni, F. Morichetti, and M. Martinelli, "Optical Slow Wave Structures," *Optics & Photonics News* **14**, 44 (2003)
14. J. Scheuer, G.T. Paloczi, J.K.S. Poon and A. Yariv, "Coupled Resonator Optical Waveguides: Toward the Slowing & Storage of Light," *Optics & Photonics News* **16**, 36 (2005).
15. H. Altug and J. Vučković, "Experimental demonstration of the slow group velocity of light in two-dimensional coupled photonic crystal microcavity arrays," *Appl. Phys. Lett.* **86**, 111102 (2005).

16. A. Melloni, F. Morichetti and M. Martinelli, "Linear and Nonlinear propagation in coupled resonator slow-wave optical structures," *Opt. and Quantum Electron.* **35** 365-379 (2003).
17. M. Ghulinyan *et al.*, "Free-standing porous silicon single and multiple optical cavities," *J. Appl. Phys.* **93**, 9724 (2003).
18. A. Galindo and P. Pascual, *Quantum Mechanics II*, (Springer, Berlin, 1991).
19. B. R. Bennett, R. A. Soref, J. A. Del Alamo, "Carrier-Induced Change in Refractive Index of InP, GaAs, and InGaAsP," *IEEE J. Quantum Electron.* **26**, 113-122 (1990).
20. A. Liu, R. Jones, L. Liao, D. Samara-Rubio, D. Rubin, O. Cohen, R. Nicolaescu, M. Paniccia, "A High-Speed Silicon Optical Modulator Based on a Metal-Oxide-Semiconductor Capacitor," *Nature* **427**, 615-618 (2004).
21. V. R. Almeida *et al.*, "All-optical switching on a silicon chip," *Opt. Lett.* **29**, 2867 (2004).
22. Y.-H. Ye *et al.*, "Finite-size effect on one-dimensional coupled-resonator optical waveguides," *Phys. Rev. E* **69**, 056604 (2004).
23. M. Ghulinyan, M. Galli, C. Toninelli, J. Bertolotti, S. Gottardo, F. Marabelli, D.S. Wiersma, L. Pavesi, L. Andreani, "Wide-band transmission of non-distorted slow waves in 1D optical superlattices," *Appl. Phys. Lett.* **88**, 241103 (2006).
24. see, e.g. C.R. Pollock, *Fundamentals of Optoelectronics* (Irwin, Chicago, 1995).
25. A.S. Sudbo, "Numerically stable formulation of the transverse resonance method for vector mode-field calculations in dielectric waveguides," *IEEE Photon. Technol. Lett.* **5**, 342-344 (1993).
26. P. Sanchis, J. Marti, W. Bogaerts, P. Dumon, D. Van Thourhout, R. Baets, "Experimental results on adiabatic coupling into SOI photonic Crystal coupled-cavity waveguides," *Photonics Technology Letters*, **17**, 1199-1201 (2005).
27. R.C. Alfemess, "Optical guided-wave devices," *Science* **234**, 825-829 (1986).

1. Introduction

Techniques for flexible and efficient all-optical wavelength conversion play a central role in many signal processing and telecommunication applications [1]. Some among the most promising techniques are based on nonlinear wave-mixing effects [2], or on optical gating techniques such as cross-gain and/or phase modulation [3]. Unfortunately, both these approaches have severe limitations concerning the tunability range of the final frequency, the efficiency of the conversion process, and preservation of the full amplitude and phase information.

Dynamical photonic structures, where the optical constants of the medium are modulated while the light is propagating inside it, have been recently introduced and are now attracting a great deal of interest from both the theoretical and experimental side (for a review, see e.g. [4]). Structures of this kind open up an intriguing research area in view of stopping, storing, and manipulating optical information [5, 6, 7].

In the present paper a possible solution to the wavelength conversion problem is proposed which makes use of a dynamical photonic structure. The photon dispersion is dynamically changed by simply changing the refractive index of the structure while the optical pulse is propagating across it, which results in an almost lossless and continuously tunable shift of the photon energy without affecting the pulse shape nor the coherence. This aspect is emphasized by referring to it as *photon energy lifter*.

2. Basic principle: frequency lift in homogeneous media

It is a simple consequence of translational invariance that the wavevector k of an electromagnetic wave propagating in a homogeneous and non-absorbing dielectric with a time-dependent refractive index $n(t)$ is a conserved quantity. As the frequency is related to the wavevector and the refractive index by $\omega = \frac{c}{n}k$, where c is the velocity of light in vacuum, a change of refractive index by δn results in a change of the frequency of a plane wave by

$$\frac{\delta\omega}{\omega} = -\frac{\delta n}{n_0 + \delta n} \simeq -\frac{\delta n}{n_0} \quad (1)$$

This effect can be used in a photonic device to shift the carrier frequency of a wave-packet (light pulse), without dramatically affecting the pulse shape. The optical linearity of the medium

guarantees that the different k -components are decoupled, so that the pulse shape is preserved in both the real and the k -space. In practice, one needs to trigger the refractive index shift once the pulse has entered the medium and to complete it before the pulse starts exiting, so that the index change occurs while the medium is *loaded with optical energy* and propagation really occurs through a time-dependent device. Otherwise, the index change would simply result in a mere modification of the transmission spectra of the device as it happens in any pump-probe experiment [8]. Note that the energy required for the frequency change is provided by the work done while changing the refractive index of the medium.

Unfortunately, the experimental implementation of this idea is very demanding for available technology. As the travel time $\tau_{travel} = L/v_g$ of the pulse across the structure must be longer than the pulse duration τ_{pulse} plus the switching time τ_{sw} , the device length L has to be longer than $L_{min} = v_g(\tau_{pulse} + \tau_{sw})$. For realistic values of τ_{pulse} and τ_{sw} of the order of a few tens of picoseconds, and group velocities v_g of the order of a significant fraction of c , L_{min} can be as long as some millimeters. Such a length it is undesirable in the perspective of miniaturization and integration.

3. Single-cavity lifter

A simple way of increasing the travel time across the structure is to use an optical microcavity [9, 10] to store the electromagnetic energy while changing the index. In this time-dependent optical microcavity approach, a possible procedure to shift the frequency is the following: a) injection of electromagnetic energy in the cavity; b) shift of the resonance frequency, e.g. by a change of refractive index; c) release of the frequency-shifted electromagnetic energy. This idea has been recently discussed in [11], but the pulse injection process and the shape of the output pulse have not been addressed in full detail. To quantitatively understand the pros and the cons of the single-cavity configuration, Finite Difference Time Domain (FDTD) simulations have been performed to fully describe the propagation of a light pulse through a single $\lambda/2$ time-dependent cavity. The results are summarized in Fig. 1 for a Distributed Bragg Reflector (DBR) cavity.

The microcavity is a fundamentally different solution with respect to the case of a homogeneous medium discussed in the previous section: light is in fact injected in a localized state, and a fundamental trade-off in the trapping capability has to be pointed out. On one hand, a high quality factor Q is required in order to have a long storage time once the cavity has been charged. This gives in fact longer time to apply the frequency shift before the optical energy is released, thus adding practical flexibility to the device implementation. On the other hand, a high quality factor means a very narrow bandwidth. This is undesirable for optical pulse processing, because the energy transfer between the incident charging wave and the cavity itself is limited to this frequency window. This results in low efficiency in the cavity charging, as well as in a strong distortion of the pulse shape, as shown in Fig. 1. Unless the pulse duration is much longer than the storage time, the energy exits in fact from the cavity as a slow, exponentially decaying wave, according to the characteristic Lorentzian filtering of the cavity, and the output peak intensity is lower than the input one by almost 2 orders of magnitude.

Two additional undesirable features are also visible in Fig. 1. First, the light exits also from the input side. This appears in the figure as a change of sign of Poynting vector at input side (dashed line) at time $\simeq 30$ ps. As implied by the symmetry of the structure, energy exits from both sides with the same amplitude (in the figure, this is partially hidden by the 30 times magnification). Second, a fraction of the stored energy unavoidably exits before the index shift (this feature is recognizable in the spectrum, as the solid bump at 1550.25 nm).

The comparison between the homogenous medium and the single cavity enlightens the path towards a solution which combines the respective advantages. A larger bandwidth than the one

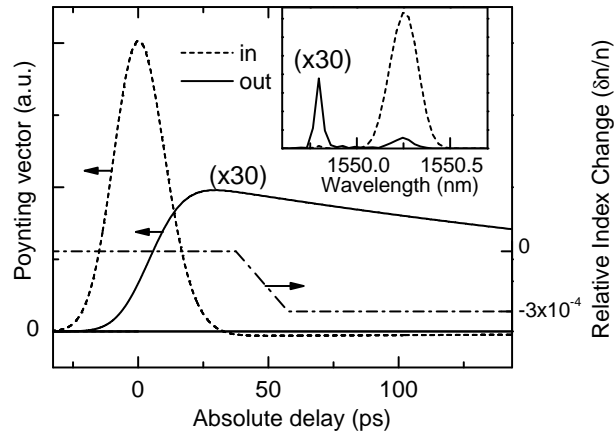


Fig. 1. Finite difference Time Domain (FDTD) simulation of the frequency shift in a sample time-dependent single Fabry-Perot microcavity. The simulated cavity, resonant at vacuum wavelength $\lambda=1550.25$ nm, consists in a $\lambda/2$ layer (thickness = 388 nm with refractive index = 2) sandwiched between two 8.5-period Distributed Bragg Reflectors, fabricated by alternating high refractive index $\lambda/4$ layers (thickness = 129 nm with refractive index = 3) and low refractive index $\lambda/4$ layers (thickness = 194 nm with refractive index = 2). A Gaussian pulse of duration 20 ps is taken as the input. The dashed (solid) line shows the amplitude of the Poynting vector at the input (output) side versus time. The inset shows the spectra of respective electric fields (the resolution of the spectrum of the output is limited by the time window of the simulation).

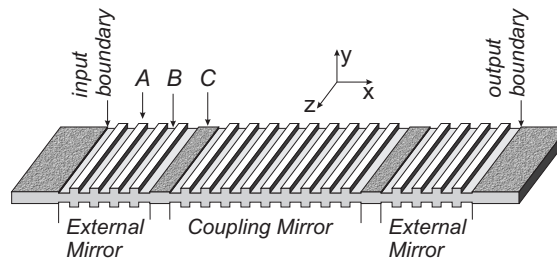


Fig. 2. Simplified schematic representation of the CROW structure. For simplicity, we have represented the external dielectric mirrors with only 4 periods instead of 13, and the inter-cavity – coupling – mirrors with only 9 periods instead of 27. Only 2 cavities instead of 45 have been shown. Light travels in the positive x direction.

provided by the single microcavity is needed for the applications, but without sacrificing the light trapping ability of optical microcavities. We achieve this goal by resorting to coupled microcavities.

4. Coupled Resonator Optical Waveguide (CROW) lifter

Various photonic systems have been recently investigated to lower the group velocity of light. Line-defect photonic crystals [12] and coupled resonator optical waveguides (CROW) [13, 14, 15] are among the most promising ones.

Here we focus our attention on the case of a CROW structure (see sketch in Fig.2), i.e. a spatially periodic many-cavity system, in which the degeneracy of the single cavity modes is

lifted by the coupling between neighboring cavities via the finite transmittivity of the mirrors. As in the previous section the mirrors are always assumed realized by DBRs. As a result, a miniband is created (left and central panels of Fig.3), whose dispersion law in the weak coupling limit (for the general expression, see, e.g., [16]) has the form:

$$\omega_0(k) = [\bar{\omega} - J \cos(k\ell)], \quad (2)$$

The miniband is centered at the single cavity frequency $\bar{\omega}$ and its width is given by the coupling J between neighboring cavities, which is proportional to the tunneling amplitude through the mirror [17]. Here, ℓ is the CROW period and the quasi-wavevector k is defined modulo integer multiples of the reciprocal lattice vector $2\pi/\ell$. As a consequence of the strong light localization in the cavity modes (Fig. 3), the group velocity is orders of magnitude lower than the one associated to the average refractive index of the structure.

A spatially uniform (x is the spatial coordinate along the structure) relative change of the refractive index of the form:

$$n(x) = (1 + \varepsilon) n_0(x) \quad (3)$$

results in a frequency shift of the miniband:

$$\omega_\varepsilon(k) = \frac{\omega_0(k)}{1 + \varepsilon} \quad (4)$$

Provided the electromagnetic field dynamics is limited to the miniband states only (adiabatic regime) [18], a variation in time of the refractive index of the form (3) implies a coherent frequency shift of the whole wavepacket according to (4), in a way analogous to the homogeneous case. The adiabatic requirement implies that the tuning time τ_{sw} be much larger than the inverse of the minimum frequency separation $1/\Delta\Omega$ between the miniband state and the nearest photonic state with the same symmetry, i.e. the same quasi-wavevector k . In Fig. 3, $1/\Delta\Omega$ can be seen to be on the order of 0.1 ps. In semiconductors, the refractive index n can be modulated, e.g., by changing the free carrier density [19]. In particular, in Si, relative index modulation of the order of $\sim 10^{-4}$ has been recently demonstrated in the GHz range [20, 21].

In the finite CROW system, the impedances can be carefully matched at the input and output interfaces, so that the central part of the miniband corresponds to a frequency window in which the transmittivity is flat and almost unity (right panel of Fig.3). If the incident pulse (dotted line in right panel) fits in this spectral region, the pulse can penetrate into the photonic structure and then travel across it. As the miniband dispersion (central panel) is almost linear in this region, no broadening nor distortion of the pulse shape occurs during propagation. As the miniband is rigidly shifted by the index change, no distortion occurs during lifting.

Quantitatively, the fact that the pulse has to be contained in the central part of the miniband imposes a lower limit to the pulse duration $\tau_{pulse} \gg 1/J$. For the parameters of the figure, $1/J \approx 1$ ps. As the travel time τ_{travel} depends on the group velocity [22], a strong reduction of v_g with respect to c implies a much looser lower bound L_{min} on the system length L in order for the refractive index modulation to be performed while the pulse is contained in the structure.

5. CROW design and FDTD simulations

Our design is based on a Si corrugated waveguide (see the sketch in Fig.2). The guide includes a Si core layer of about 260 nm thickness, sandwiched between SiO₂ cladding layers. The index contrast between the two materials assures light confinement in the Si core. The photonic structure is realized by modulating the thickness of the Si slab. The design consists in 45 Fabry Perot microcavities, coupled by 27-period DBRs. The DBRs and cavities are constituted by quarter- and half-wavelength layers, respectively, and are centered at $\lambda_0 = 1550$ nm. The modulation of the Si core thickness is designed to achieve – for the fundamental transverse mode –

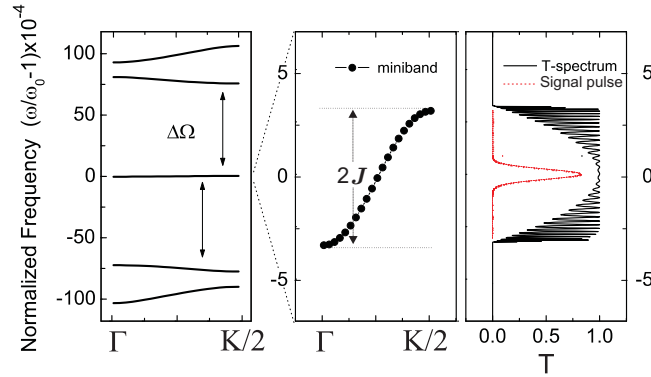


Fig. 3. Left panel: band structure of the 1D model of the CROW structure shown in Fig.2. The arrows indicate the frequency separation $\Delta\Omega$ between the miniband and the nearest photonic states with the same k . Central panel: enlarged view of miniband. Right panel: transmission spectrum and spectral shape of the signal pulse. This latter is chosen to fit in the region of the spectrum where the dispersion is linear and the transmittivity is flat and almost unity. Vertical axes have all the same (dimensionless) unit. For the actual parameters see text.

the effective index values $n_A = 3$, $n_B = 2.426$ and $n_C = 2.688$, respectively, for the high-index layer (A) of the DBRs, the low-index layer (B) of the DBRs, and the cavity layer C. These effective parameters have been used in the 1D FDTD simulations of Figs.3 and 4.

The time dependence of the structure consists of a refractive index change of the Si core originating due to the presence of optically or electrically injected carriers. In the simulations, this is modelled as a spatially homogeneous relative shift $\varepsilon(t) = \delta n(x,t)/n_0(x)$ of the refractive index of each layer, triggered after the injection of the pulse and completed before the pulse exits. For simplicity, a linear time dependence of $\varepsilon(t)$ has been considered. The number of cavities has been determined by the constrain that the pulse must be contained inside the structure during the time required for the index switch, assumed to be 20 ps. The final device length is about 370 μm . A slower switching time would simply imply a proportionally higher number of cavities and a correspondingly longer structure. Note that the minimum tuning time τ_{sw} for being adiabatic is, for our parameters, of the order of 0.1 ps, i.e. orders of magnitude shorter than the switching time of most existing materials. A value $\delta n/n_0 = -3 \times 10^{-4}$ has been used for the relative refractive index shift that can be induced e.g. by creating free carriers in the Si material either electrically [20] or optically by means of an extra laser at shorter wavelength [21]. In the former case, the needed electrical energy to create the required carrier density in the whole volume of the structure is of the order of some nJ, whereas in the latter case, the needed optical energy turns out to be the order of some 100 pJ.

The results of the FDTD simulation of the pulse propagation are reported in Fig. 4. The pulse delay is 116 ps, i.e. a factor $\simeq 35$ larger than what expected in a homogeneous structure with the same length and same average refractive index. The distortion of the input pulse is negligible¹ and the efficiency of conversion is larger than 95%. The resulting vacuum wavelength shift $2\pi c/\delta\omega = -\delta\lambda \simeq -0.49$ nm perfectly matches the expected value $\delta\lambda/\lambda_0 \simeq |\delta n/n_0| = 3 \times 10^{-4}$. This simple scaling law anticipates that a much wider tuning range is possible, just by

¹Optical path imperfections of the cavities can result in reshaping of the miniband (breaking the spectrum symmetry against the central frequency). The latter can result in appearance of small transmission bumps at the miniband edges which can lead to a distorted or oscillatory pulse output. Such a problem however is not too severe, provided that the input pulse fits into the flatter part of the miniband.[23]

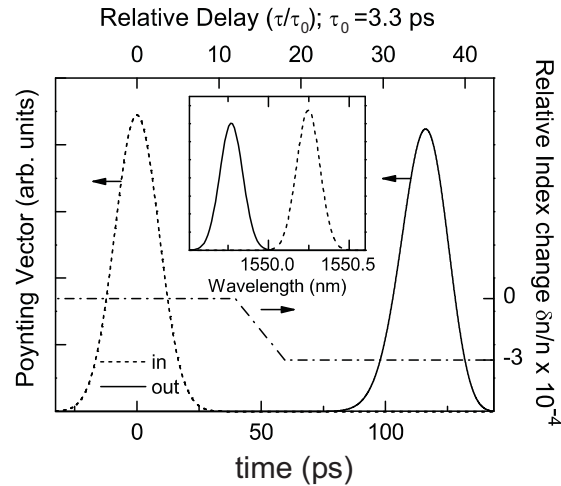


Fig. 4. FDTD simulation of the envelope of Poynting vectors at the input (dashed line, positive entering) and output boundary (solid line, positive exiting) of the coupled-cavities structure. Input and output boundaries are defined in Figure 2. The refractive index of all the layers is time-dependent, as shown by the right y-axis. Upper time scale is relative to the delay (τ_0) in a homogeneous medium with the average refractive index of the 1D-structure. The inset shows the spectra of the input and output pulse electric fields.

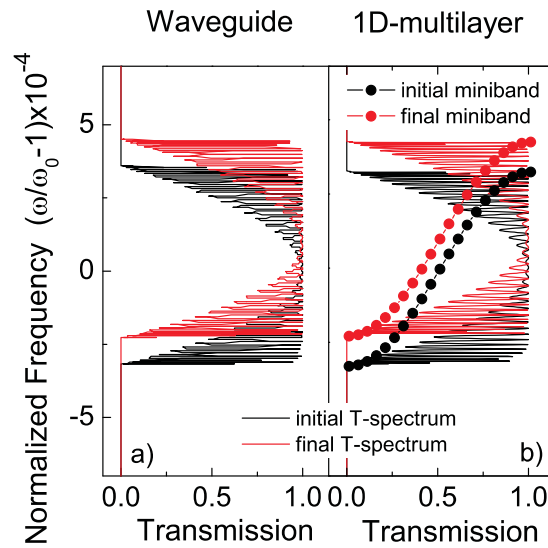


Fig. 5. (color online) A comparison between the calculated transmission spectra of the initial and shifted minibands in the case of a waveguide (a) and a 1D-multilayer structure (b). The miniband dispersion (full circles) in the 1D case is also plotted in (b).

resorting e.g. to electro-optic materials like LiNbO_3 [24] for which $\delta n/n_0$ can be as high as 10^{-3} or larger.

Even though the FDTD simulation is performed on 1D time-dependent structure, the results are essentially applicable also to the quasi-1D slab waveguide structure of Fig. 2. This can be

demonstrated by a full (time independent) 2D simulation for the slab waveguide, performed using an eigenmode expansion method [25]. We assume a vertical symmetric (the y -direction) architecture, as sketched in Fig. 2. The physical parameters of the integrated device (length and thickness of the layers) have been chosen in order to maintain a good modal matching between input/output waveguides, cavities and DBRs. In this way the insertion losses in the resulting two dimensional CROW slab device appear to be negligible, of the order of 0.1dB. In Fig. 5 the miniband spectra of the slab structure (panel (a)) and the 1D model of the CROW (panel (b)) are shown both at the initial time and after the spatially homogeneous relative shift of refractive index. The close similarity of the two graphs confirms that the 1D model and the corresponding 1D FDTD simulations provide an accurate description of light propagation through the slab waveguide system and of the predicted photonic lift effect.

We remark that our 1D and 2D models do not take into account losses related to 3D effects, which might lead to significant degradation in terms of the device efficiency. However, we expect loss optimization to be more effective in quasi-1D structures (which is the case discussed here) than in quasi-2D structures. [26]

6. Travelling wave design

Up to now the basic idea of the photon energy lifter was based on the hypothesis that the refractive index can be changed at the same time in the whole structure while the pulse is travelling across it. Another possible scheme, which can simplify the experimental realization is what can be called a travelling-wave design [27]. In this scheme, the electrical field for the electro-optic effect is not applied simultaneously to the whole device, but is injected as a microwave from one end of the electrode pair. Electrodes work as a transmission line. In this design, the electrode capacitance, being distributed, does not limit the modulator speed, and the electrodes can be made very long.

Since the photonic structure under study is designed for *optical* wavelengths, it behaves as a homogeneous medium at microwaves. Therefore, it is expected that the group velocity at microwaves is determined by the average refractive index, $n_{\mu w}$, of the structure and thus it is much higher than the group velocity of the optical pulse. Moreover, the optical wavelength $\lambda \simeq 1.55 \mu\text{m}$ being much shorter than the thickness of the microwave rise front L_{rise} , the optical pulse sees an almost translationally invariant system with a time-dependent refractive index.

In order to verify that no spurious effect occur at the microwave front, we have performed 1D FDTD simulations for the coupled microwave and optical pulses. In the FDTD simulations, we assume a conservative value of $n_{\mu w}=3$ for the effective refractive index of the mixed Si/SiO₂ structure at microwaves: the optical group velocity v_g in our structure is therefore lower than the microwave group velocity $c/n_{\mu w}$ by over an order of magnitude. The microwave driver signal is taken as a smooth function $\propto (1 - \exp(-t/\tau))$ with $\tau^{-1} = 100\text{GHz}$, long enough for $L_{rise} = c/\tau = 3 \cdot 10^{-3} \text{m} \gg \lambda$. The microwave is sent into the structure with a 35 ps delay from the input light signal, i.e., when the injection of the light signal is essentially completed (Fig. 4). Sample electric field snapshots resulting from the combined optical and microwave simulations are reported in Fig. 6, where an instantaneous response of the refractive index to the microwave amplitude has been assumed. The results of the travelling-wave simulation are not distinguishable from the results of Fig. 4, which verifies the effectiveness of this second travelling wave scheme to shift the pulse carrier frequency.

7. Conclusions

We have proposed a novel photonic device which is able to shift the carrier frequency of an optical pulse without affecting its shape nor its coherence. The efficiency of the process is not affected by any fundamental effect, and has been shown by our simulations to be close to one.

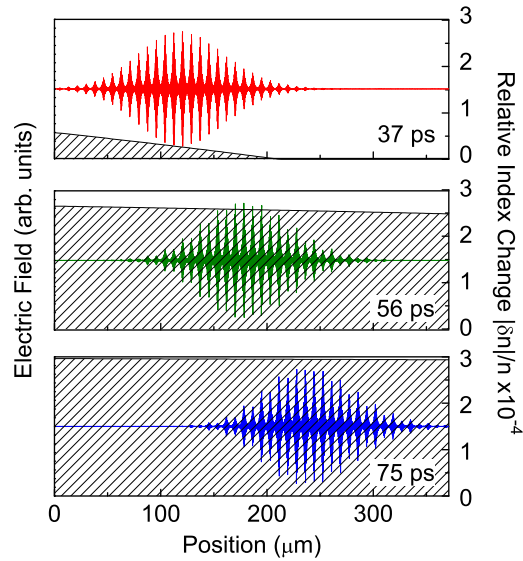


Fig. 6. (color online) Successive snapshots of the electric field of the optical wave and of the index-driving microwave at 37, 56 and 75 ps. The differently colored electric fields have an illustrative scope and refer to a blueshift of the input pulse wavelength. The structure of the pulse electric field reflects the coupled cavity structure (maxima are located in correspondence of C layers).

The relative frequency shift is equal to the relative refractive index change in the material and can therefore be tuned in a continuous way. All these features suggest that our scheme may have a significant impact on applications which require all-optical transmission and processing of classical and even quantum information.

We acknowledge the financial support by MIUR through FIRB (RBNE01P4JF and RBNE012N3X) and COFIN (2004023725) projects and by PAT through PROFILL project.